(13) Lindemann, L. P.; Adams, J. Q. *Anal. Chem.* **1971**, *43*, 1245.
(14) Natta, G.; Giachetti, E.; Pasquon, I.; Pajaro, G. *Chim. Ind. (Milan)* **1960**, *42*, 1091.
(15) Miyazawa, T.; Ideguchi, T. *J. Polym. Sci., Part B* **1963**, *1*, 389.
(16) Zambelli, A.; Giongo, M. G.; Natta, G. *Makromol. Chem.* **1968**, *112*, 183.
(17) Lazzaroni, R.; Salvadori, P.; Pino, P. *J. Organomet. Chem.* **1972**, *43*, 233.
(18) Ammendola, P.; Ciajolo, M. R.; Panunzi, A.; Tuzi, A. *J. Organomet. Chem.* **1983**, *254*, 389.
(19) Stefani, A.; Tatone, D.; Pino, P. *Helv. Chim. Acta* **1979**, *62*, 1098.

Studies on Stereospecific Sequence Distributions in Polypropylenes by Pyrolysis–Hydrogenation Fused-Silica Capillary Gas Chromatography

Hajime Ohtani and Shin Tsuge*

Department of Synthetic Chemistry, Faculty of Engineering, Nagoya University, Furo-cho, Chikusa-ku, Nagoya 464, Japan

Toshio Ogawa† and Hans-Georg Elias

Michigan Molecular Institute, Midland, Michigan 48640. *Received May 16, 1983*

ABSTRACT: The stereoregularity of various polypropylenes (PP's) has been studied by pyrolysis–hydrogenation gas chromatography with a high-resolution fused-silica capillary column. On the basis of the pyrograms obtained, average stereoregularity and stereospecific sequence length of PP's were estimated from the relative intensities among the tetramer peaks and the pentamer peaks, respecitvely. Peak intensities of the larger products were also in harmony with the estimated stereospecific sequence length. The relative peak intensities of the C_{10}-trimer peaks were used in the estimation of the degree of chemical inversion of the monomer units along the polymer chain. As a result, it was found that most of the chemical inversions were present in the syndiotactic sequences. The mechanism of the stereoisomerization accompanied by pyrolysis of PP's is also discussed.

Polypropylene (PP) is a typical stereoregular polymer, and its physical properties are affected not only by the average molecular weight and the molecular weight distribution but also by the configurational characteristics. Until now structural characterization of PP's has been carried out mainly by X-ray diffraction, IR, and NMR. The ^{13}C NMR spectra of the methyl carbons, which are clearly split corresponding to the tactic pentad placement, have been extensively applied to the determination of the stereoregularity (tacticity) of PP's in recent years.[1-4]

Pyrolysis–gas chromatography (PGC) has been also applied to the characterization of PP. Tsuchiya et al.[5] investigated the pyrolysis of isotactic PP in vacuum at around 400 °C and suggested that intramolecular transfer of secondary radicals played an important role in the degradation mechanism. Audisio et al.[6] studied stereoirregular, isotactic, and syndiotactic PP's without hydrogenation and identified some diastereoisomeric components of the tetramer fraction. The relative intensities of the diastereoisomers reflected the tacticities of the decomposed polymer. In contrast, Seeger et al.[7] made use of PGC with in-line hydrogeneation (PHGC) and achieved fairly good separation of the diastereoisomeric fragments of PP's with various tacticities. However, they pointed out that the configuration in the fragments differs from that in the original chain because of isomerization during thermal degradation and suggested that the isomerization was caused mainly by stepwise transfer of the radicals in the cyclization process. As a result of PGC with a gas density detector, Kiran et al.[8] attributed the major pyrolysis products of PP to intramolecular radical transfers in the secondary macroradicals to the 5th, 9th, and 13th carbon atoms and those in the primary macroradicals to the 6th, 10th, and 12th carbon atoms. Kiang et al.[9] and Dickens[10] investigated the kinetics and mechanism of the thermal degradation of PP's.

Recently, PHGC with a high-resolution glass capillary column has been applied to the configurational characterization of PP's.[11] The assigned characteristic peaks of tetramers (C_{11}–C_{13}) and pentamers (C_{14}–C_{16}), which reflect tactic dyads and triads, respectively, were interpreted in terms of the average stereoregularity, whereas the peaks of C_{10}-trimers were applied to the elucidation of the degree of chemical inversion of the monomer units.

In this work, the PHGC technique was modified by incorporating a fused-silica narrow-bore capillary column to obtain further improvement in the resolution of the pyrograms up to tridecamers (C_{38}–C_{40}), which reflect the longer stereospecific sequences. On the basis of the observed high-resolution pyrograms of various PP's differing in stereoregularity, the stereospecific sequence length was estimated along with the average stereoregularity. In addition, the relation between the degree of chemical inversion and stereoregularity was studied. The mechanism of the stereoisomerization accompanied by pyrolysis of PP's is also discussed in terms of intramolecular radical-transfer processes.

Experimental Section

Samples. The raw material for the predominantly isotactic PP (iso-PP) was synthesized in the presence of a typcial Ziegler–Natta catalyst, $AlEt_2Cl/TiCl_3$. PP-I(A) was prepared by removing the amorphous portions from the raw material through *n*-hexane extraction. The diethyl ether soluble fraction of the raw material was used as PP-I(B), which was expected to be mainly composed of atactic-PP (atac-PP). Predominantly syndiotactic PP (synd-PP) prepared in the presence of $AlEt_2Cl/VCl_4$ was used as PP-II. These three PP samples are the same as those used in the previous work.[11] Another raw material of PP with syndiotactic stereoblocks was synthesized in the presence of

† Present address: Hirakata Plastics Laboratory, Ube Industries Ltd., Hirakata, Osaka 573, Japan.

0024-9297/84/2217-0465$01.50/0 © 1984 American Chemical Society

Table I
Polypropylene Samples

polymer	preparative conditions
PP-I(A)	$AlEt_2Cl/TiCl_3$ catalyst, *n*-hexane extracts removed residue
PP-I(B)	$AlEt_2Cl/TiCl_3$ catalyst, diethyl ether extracts
PP-II	$AlEt_2Cl/VCl_4$ catalyst
PP-III(A)	$AlEt_2Cl/VCl_4$/anisole catalyst, diethyl ether extracts (extraction I)
PP-III(B)	hexane extracts of the residue in extraction I (extraction II)
PP-III(C)	heptane extracts of the residue in extraction II (extraction III)
PP-III(D)	the residue in extraction III

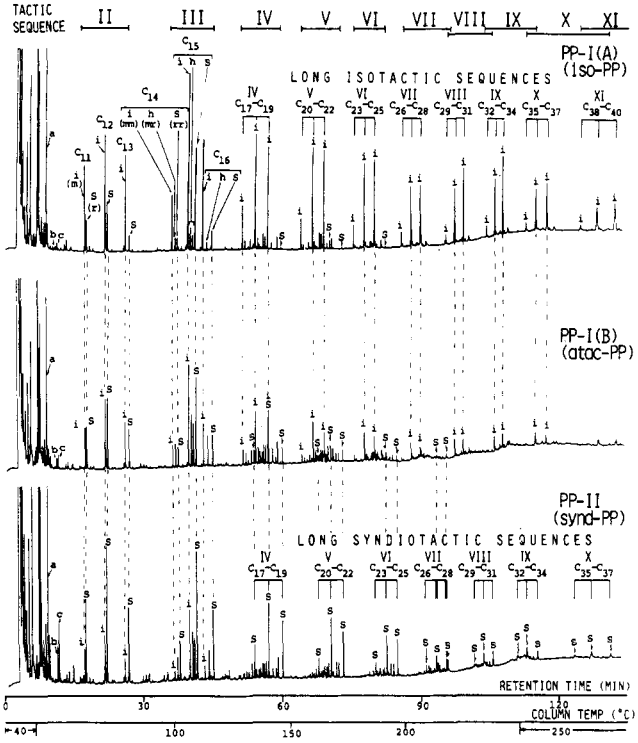

Figure 1. High-resolution pyrograms of PP-I(A), PP-I(B), and PP-II; i, s, and h represent isotactic, syndiotactic and heterotactic products, respectively; a, b, and c are C_{10} trimers used to calculate the chemical inversions by eq 8.

$AlEt_2Cl/VCl_4$/anisole at −78 °C.[12] From this raw material, PP-III(A)–PP-III(D) were prepared by the successive fractional extractions with diethyl ether, hexane, and heptane. The PP samples examined in this work are listed in Table I along with the preparative conditions.

Conditions for PGC. The pyrolysis–hydrogenation capillary gas chromatographic system utilized in this work is basically the same as that described previously.[13] A vertical microfurnace-type pyrolyzer (Yanagimoto GP-1018) was directly attached to a gas chromatograph (Shimadzu 7AG) with a fused-silica narrow-bore capillary column (0.32-mm o.d. × 0.2-mm i.d. × 50-m long) the wall of which was coated with OV-101 supplied by Hewlett-Packard. A small piece of precut column (3-mm i.d. × 5-cm long) containing 5 wt % of OV-101 packing (80/100 mesh Diasolid-H) and a hydrogenation catalyst column (3-mm i.d. × 10-cm long) containing 5 wt % of Pt packing (80/100 mesh Diasolid-H) were inserted in series between the pyrolyzer and a splitter with a splitting ratio of 1:40. Both the precut column and the catalyst column were maintained at 200 °C. The precut column was used to protect the catalyst and the separation column from tarry and/or less volatile degradation products. The column temperature was programmed from 40 to 250 °C at a rate of 2 °C/min after maintaining 40 °C for 4 min. A sample of about 300 μg was pyrolyzed at 650 °C under a flow of hydrogen carrier gas (40 mL/min).

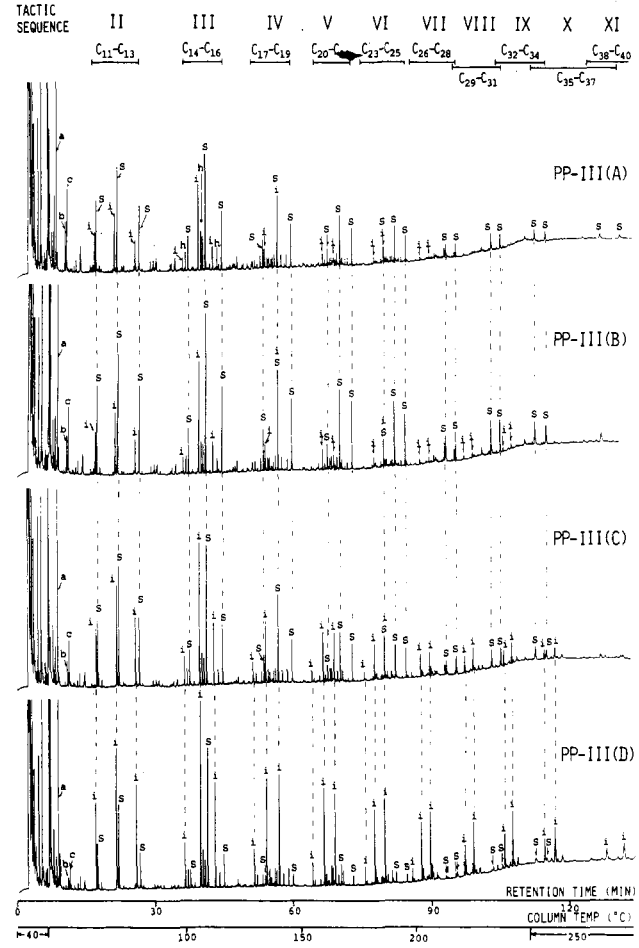

Figure 2. High-resolution pyrograms of PP-III series; i, s, and h, and a, b, and c are the same as in Figure 1.

Results and Discussion

Stereospecific Sequence Length. Figures 1 and 2 show the high-resolution pyrograms of PP-I(A), PP-I(B) and PP-II, and PP-III series, respectively. The tetramer (C_{11}–C_{13}) peaks are composed of a triplet of doublets which corresponds to an isotactic dyad (m = meso) and syndiotactic dyad (r = racemic) pair. On the other hand, the pentamer (C_{14}–C_{16}) cluster consists of 10 clearly separated peaks which retain isotactic, heterotactic, and syndiotactic triads corresponding to mm, mr, and/or rm and rr, respectively.[11] The relative peak intensities of these characteristic diastereoisomers reflect the original stereoregularities along the polymer chain although they do not always correspond to the exact values because of the thermal isomerization during pyrolysis at high temperatures.[5–11]

Table II summarizes the quantitative data for the C_{11}–C_{13} tetramer doublets on the pyrograms and the ^{13}C NMR determined from the configurational dyad content.[12] Here, the relative peak intensity was defined as follows:

$$\% \text{ m} = \frac{I_m}{I_m + I_r} \times 100 \quad (1)$$

$$\% \text{ r} = 100 - \% \text{ m} \quad (2)$$

where I_m and I_r are the peak intensities of the m peak and r peak for a give dyad doublet, respectively. Of the three dyad doublets, the C_{13} dyads, both end groups of which are isopropyl groups, are always most characteristic of the original stereoregularity. Thus, the data suggest that PP-I(A) is highly isotactic and that P-II is highly syndiotactic while PP-I(B) is between them. On the other hand, the data for the PP-III series suggest that quite significant

Table II
Relative Peak Intensities between Dyad Doublet

sample	C_{11}		C_{12}		C_{13}		^{13}C NMR[a]	
	% m	% r	% m	% r	% m	% r	% m	% r
PP-I(A)	70.0	30.0	77.7	22.3	88.2	11.8	95.4	4.6
PP-I(B)	47.2	52.8	47.9	52.1	52.7	47.3		
PP-II	25.8	74.2	25.1	74.9	20.4	79.6		
PP-III(A)	31.8	68.2	33.8	66.2	28.9	71.1		
PP-III(B)	31.3	68.7	29.9	70.1	26.2	73.8	26.5	73.5
PP-III(C)	43.6	56.4	48.7	51.3	50.2	49.8	49.1	50.9
PP-III(D)	62.4	37.6	67.7	32.3	76.8	23.2		

[a] The relative intensity of configurational dyads was calculated from the relative intensity of triads for the methyl carbon. That is % m = % mm + $^1/_2$(% mr) and % r = % rr + $^1/_2$(% mr).

Table III
Relative Peak Intensities between Triad Peaks

sample	C_{14}			C_{15}			C_{16}			^{13}C NMR		
	mm	mr	rr	mm	mr	rr	mm	mr	rr	mm	mr	rr
PP-I(A)	66.7	19.0	14.4	62.8	8.3	28.8	82.1	5.4	12.5	93.5	3.7	2.8
PP-I(B)	35.6	37.1	27.2	38.1	32.1	29.8	42.1	28.2	29.8			
PP-II	12.1	32.2	55.7	22.8	29.3	47.9	11.3	24.7	64.0			
PP-III(A)	19.3	28.0	52.7	30.2	23.3	46.6	21.6	20.9	57.5			
PP-III(B)	19.9	21.3	58.8	32.4	15.7	52.0	22.9	11.3	65.8	17.6	17.8	64.6
PP-III(C)	35.8	23.3	40.9	43.3	14.6	42.2	45.1	11.7	43.3	42.0	14.2	43.8
PP-III(D)	56.3	22.6	21.0	54.9	12.7	32.6	71.1	10.2	18.7			

stereospecific fractionation is attained, ranging from highly syndiotactic to highly isotactic.

The quantitative data for the tactic triads (C_{14}–C_{16} pentamers) are shown in Table III together with the ^{13}C NMR data. Here, the relative peak intensity, for example % mm, is defined as follows:

$$\% \text{ mm} = \frac{I_{mm}}{I_{mm} + I_{mr} + I_{rr}} \times 100 \qquad (3)$$

where I_{mm}, I_{mr}, and I_{rr} are the peak intensities of mm, mr (plus rm), and rr peaks, respectively. The % mr and % rr can be similarly defined. In this case, the C_{16} triads, which also have two isopropyl end groups, are the most characteristic of the original configurational structures.

It is very interesting to note that PP-I(B) has much higher % mr values than PP-III(C) (28.2 and 11.7% in C_{16} region, respectively) while their % m values in Table II are almost comparable (52.7 and 50.2% in C_{13} region, respectively). Figure 3 illustrates the detailed portions of the related pyrograms for PP-I(B) and PP-III(C). From the data of dyads (Table II), PP-III(A) and PP-III(B) should have comparably high syndiotactic structures. However, as illustrated in Figure 4, the peak intensity of the heterotactic triads (mr) for PP-III(A) is stronger than that for PP-III(B) (20.9 and 11.3% in C_{16} region, respectively). These data suggest that both the average isotactic and the average syndiotactic sequence lengths for PP-III(C) and PP-III(B) are higher than those for PP-I(B) and PP-III(A), respectively. Furthermore, PP-II exhibits the highest syndiotactic nature of all PP samples. Nevertheless, its % mr value (24.7% in C_{16} region) is greater than those of both PP-III(A) and PP-III(B) since the latter have a longer tactic sequence. On the other hand, PP-III(D) (extraction residue) has a highly isotactic nature. However, when compared with PP-I(A), it still retains relatively long syndiotactic sequences.

The number average sequence length in propylene units can be calculated from the following relationship between dyads and triads[14]

$$\bar{N}_s = 2(\% \text{ r})/\% \text{ mr} \qquad (4)$$

$$\bar{N}_i = 2(\% \text{ m})/\% \text{ mr} \qquad (5)$$

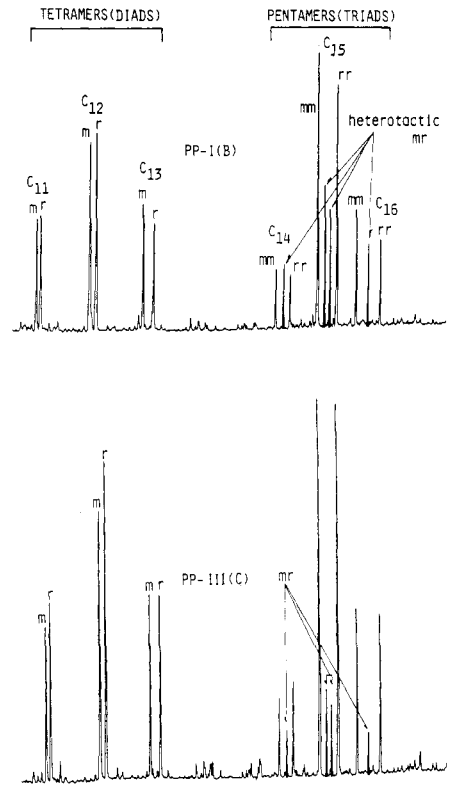

Figure 3. Detailed pyrograms of PP-I(B) and PP-III(C) for tetramer (C_{11}–C_{13}) and pentamer (C_{14}–C_{16}) regions.

where $\bar{N}_s$ and $\bar{N}_i$ are the average syndiotactic and isotactic sequence length, respectively. Table IV summarizes the values of $\bar{N}_s$ and $\bar{N}_i$ obtained by this method using the data for C_{13} dyads and C_{16} triads together with the corresponding data by ^{13}C NMR.[12] The values obtained by this method and by ^{13}C NMR are fairly comparable in spite of the fact that the stereoisomerization during pyrolysis was not taken into consideration in this method.

We now discuss the peaks of long tactic sequences beyond tetrad (IV = C_{17}–C_{19} hexamer). As shown in Figures 1 and 2, among various diastereoisomeric peaks with a given carbon number, a peak associated with an isotactic

Table IV
Number Average Syndiotactic Sequence Length ($\bar{N}_s$) and Isotactic Sequence Length ($\bar{N}_i$) Obtained by PHGC and ^{13}C NMR

	PHGC		^{13}C NMR	
sample	$\bar{N}_s$	$\bar{N}_i$	$\bar{N}_s$	$\bar{N}_i$
PP-I(A)	4.4	32.7	2.5	51.8
PP-I(B)	3.4	3.7		
PP-II	6.5	1.7		
PP-III(A)	6.8	2.8		
PP-III(B)	13.1	4.6	8.3	3.0
PP-III(C)	8.3	8.4	7.2	6.9
PP-III(D)	4.6	15.1		

sequence always has a shorter retention time than that for a syndiotactic sequence, while peaks with atactic sequences are intermediate. On the pyrogram of PP-I(A), strong chracteristic triplet peaks for long isotactic sequences up to undecads (XI) are observed. In contrast, the peaks associated with syndiotactic sequences become negligibly small above the tetrad region. These data suggest that PP-I(A) has fairly long isotactic sequences. Similarly, on the pyrogram of PP-II (synd-rich PP), characteristic triplet peaks with long syndiotactic sequences can be seen up to decads (C_{35}–C_{37} dodecamers). In this case, however, the intensity of the triplets at higher carbon numbers decay rapidly, and instead atactic multiplets are observed at the higher carbon number regions. These data indicating that the average syndiotactic sequence length of PP-II is shorter than the average isotactic sequence length of PP-I(A) are compatible with the results in Table IV ($\bar{N}_i$ = 32.7 for PP-I(A) and $\bar{N}_s$ = 6.5 for PP-II). On the pyrogram of PP-I(B) (atac-PP), complex atactic multiplets are observed up to longer sequence regions. Among PP-III series, PP-III(B) yields the strongest intensity for the peaks associated with long syndiotactic sequences, while PP-III(D) gives fairly strong peaks with long isotactic sequences. These facts are also consistent with the results in Table IV.

In order to deal quantitatively with the stereoblock length as measured by pyrograms of various PP's, a new index, syndiotactic index ($I_s(n)$), is defined using the syndiotactic C_{13} tetramer (dyad) as a reference peak as follows:

$$I_s(n) = I_s(n\text{-ad})/I_s(C_{13}) \quad (6)$$

where $I_s(C_{13})$ and $I_s(n\text{-ad})$ are the peak intensities of the C_{13} tetramer and the syndiotactic n-ad (for example, n = 3 corresponds to triad), respectively. Table V summarizes the observed $I_s(n)$ data up to the nonad (n = 9) together with the data of number average syndiotactic sequence length ($\bar{N}_s$) in Table IV. It is apparent that PP's with the higher $\bar{N}_s$ values show the greater $I_s(n)$ up to higher orders (longer sequences).

Similarly, an isotactic index ($I_i(n)$) is defined as follows:

$$I_i(n) = I_i(n\text{-ad})/I_i(C_{13}) \quad (7)$$

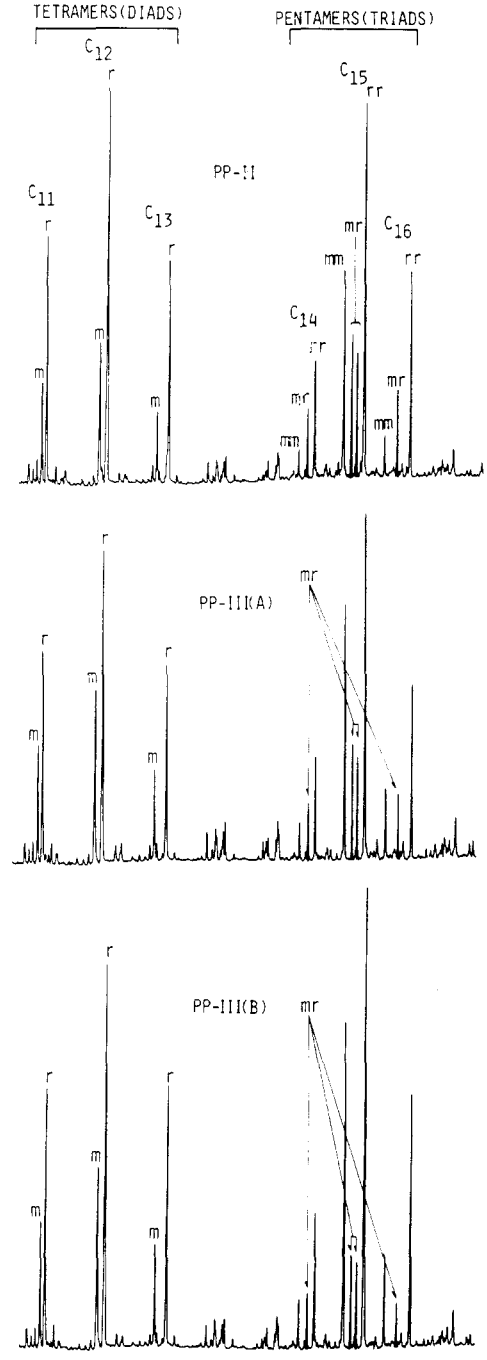

Figure 4. Detailed pyrograms of PP-II, PP-III(A), and PP-III(B) for tetramer (C_{11}–C_{13}) and pentamer (C_{14}–C_{16}) regions.

where $I_i(C_{13})$ and $I_i(n\text{-ad})$ are the peak intensities of the isotactic dyad (C_{13} tetramer) and the isotactic n-ad. Table VI summarizes the results. In this case, the values of $I_i(n)$ also correspond well to the $\bar{N}_i$ values except for PP-I(B). Although the values of $\bar{N}_i$ and $\bar{N}_s$ for PP-I(B) are almost

Table V
Relationships between Number Average Syndiotactic Sequence Length ($\bar{N}_s$) and Syndiotactic Index ($I_s(n)$)

	$I_s(n)$						
sample	n = 4	n = 5	n = 6	n = 7	n = 8	n = 9	$\bar{N}_s$[a]
PP-I(A)		0.45					4.4
PP-I(B)	0.58	0.55	0.33	0.20			3.4
PP-II	1.33	1.06	0.79	0.60	0.36	0.24	6.5
PP-III(A)	1.34	1.14	0.86	0.70	0.69	0.57	6.8
PP-III(B)	1.64	1.47	1.19	1.06	1.13	0.95	13.1
PP-III(C)	1.29	1.29	0.94	0.88	0.91	0.76	8.3
PP-III(D)	0.71	0.89	0.48	0.64	0.41	0.40	4.6

[a] The same as those by PHGC in Table IV.

Table VI
Relationships between Number Average Isotactic Sequence Length ($\bar{N}_i$) and Isotactic Index (I_i (n))

sample	I_i (n)								$\bar{N}_i$[a]
	n = 4	n = 5	n = 6	n = 7	n = 8	n = 9	n = 10	n = 11	
PP-I(A)	2.07	1.86	1.60	1.65	1.57	1.57	1.52	1.31	32.7
PP-I(B)	1.86	1.56	1.00	0.89	0.76	0.72	0.69		3.7
PP-II	0.53	0.32							1.7
PP-III(A)	1.04	0.76	0.30						2.8
PP-III(B)	1.27	0.88	0.56	0.28	0.35	0.36	0.38		4.6
PP-III(C)	1.84	1.39	1.25	1.08	0.91	0.85	0.59		8.4
PP-III(D)	1.95	1.77	1.54	1.56	1.36	1.28	1.16	0.72	15.1

[a] The same as those by PHGC in Table IV.

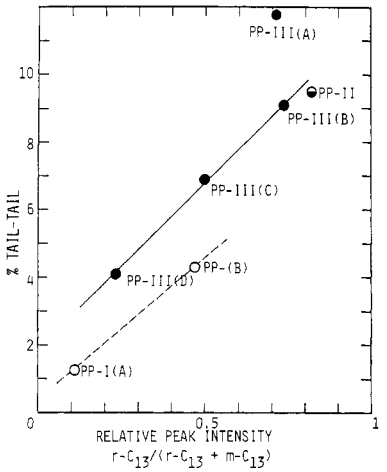

Figure 5. Relationships between the observed % tail-to-tail of various PP's and the % r in Table II.

comparable, the values of $I_i(n)$ are much greater than those of $I_s(n)$ for every n-ad. These data suggest that PP-I(B) contains small amounts of iso-PP oligomers since it was extracted from predominantly isotactic PP.

Relationship between Stereoregularity and Chemical Inversions. As was discussed in the previous paper,[11] the positional isomers in the trimer region (C_8–C_{10}) were characteristic of the enchainment of the monomer units along the polymer chain. For example, in the C_{10}-trimer region the b and c peaks on the pyrograms of Figure 1 and 2, which are 2,4-dimethyloctane and 2,5-dimethyloctane plus 3,5-dimethyloctane, respectively, correspond to tail-to-tail structures, while the main peak of C_{10} trimer (peak a, 2,4,6-trimethylheptane) represents successive head-to-tail structures. From the relative intensities of these peaks the chemical inversions in PP's can be estimated by the following equation:

$$\% \text{ tail-to-tail} = \frac{I_b + I_c}{I_a + I_b + I_c} \frac{1}{3} \times 100 \qquad (8)$$

where I_a, I_b, and I_c are peak intensities of the corresponding peaks.

Figure 5 shows the relationships between the observed % tail-to-tail for the various PP's and the % r in the C_{13} tetramer, which is a measure of its syndiotactic nature. From these data, it is apparent that the PP's prepared with the vanadium-based catalyst system(●,◒) have many more chemical inversions than those prepared with the titanium-based catalyst system(○) when compared at an equivalent tacticity.

These results can be interpreted in terms of the polymerization mechanism. In the presence of the titanium-based heterogeneous catalyst, a propylene monomer unit is added to a growing chain end at the primary metal–carbon bond by primary insertion and the successive isotactic propagation occurs mainly under the influence of the asymmetry of the catalyst sites.

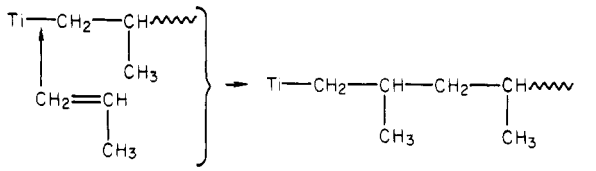

The stronger the stereospecific control by the catalyst, the higher the isotacticity and the fewer the irregular linkages attained in PP-I(A).

In the presence of the vanadium-based homogeneous catalyst, on the other hand, predominantly syndiotactic sequences are formed through secondary insertion of monomer at the secondary metal–carbon bond as the last unit in the growing chain is asymmetric.[15,16]

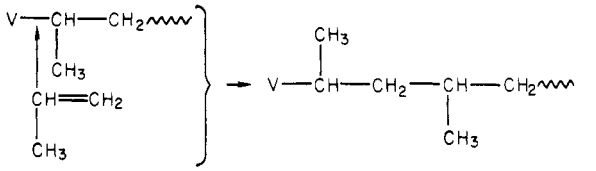

However, the primary insertion of the monomer unit also takes place to some extent to form a head-to-head linkage because the stereospecific control by the last unit is weaker than that by the Ti catalyst.

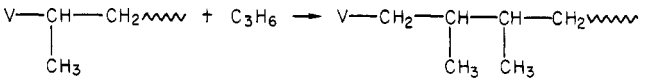

Conversely, the secondary insertion at the primary metal–carbon bond results in a tail-to-tail arrangement.

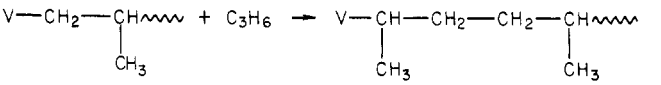

Therefore, the PP's formed with the vanadium-based catalyst have fairly large amounts of irregular linkages. Furthermore, the primary insertion at the primary metal–carbon bond results not only in isotactic propagation but also in nonstereospecific propagation because of the weak stereospecific control by the homogeneous vanadium catalyst.

In addition, it is very interesting to note that the extent of chemical inversion for the stereoblock PP's (PP-III(B), -III(C), and -III(D)) increases with the increase in syndiotactic content. This fact suggests that the majority of chemical inversions occur in the syndiotactic portions. On the other hand, the catalytic control with isotactic-specific propagation yields mostly regular head-to-tail linkages.

It is also interesting to note that PP-III(A) involves a larger extent of chemical inversion than PP-III(B) in spite of their comparable syndiotacticity. The data for the number average tactic sequence length in Table IV, how-

Scheme I

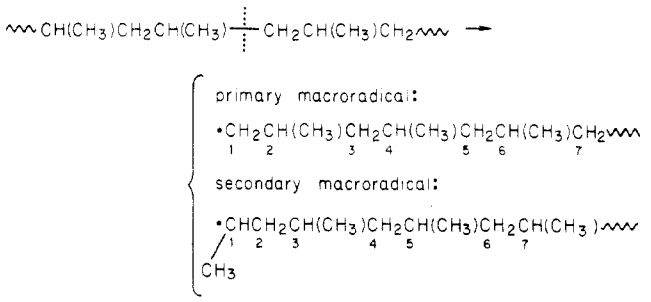

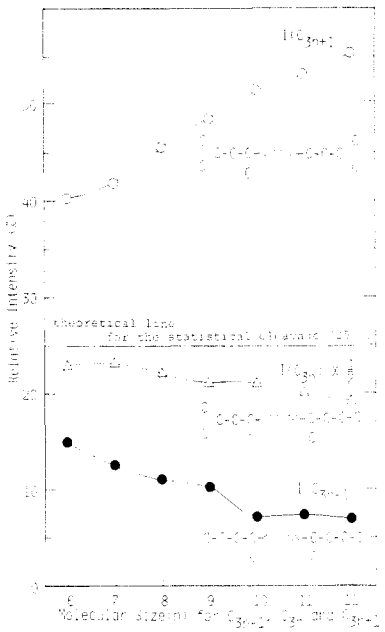

Figure 6. Relative peak intensities among isotactic fragments of C_{3n-1}, C_{3n}, and C_{3n+1} for PP-I(A) as a function of molecular size; $I(C_{3n-1}) + I(C_{3n}) + I(C_{3n+1}) = 100\%$.

ever, show that the stereoblock length for PP-III(B) in both the isotactic and syndiotactic sequence is higher than that of PP-III(A). These data imply that irregularities of the monomer insertion as well as those of tacticity are likely to take place when the stereospecific control is weak. This phenomenon also agrees with the result in our earlier work[17] where much more chemical inversions were found in atactic portions of PP's than in isotactic portions.

Mechanism of Stereoisomerization Accompanied by Pyrolysis. As was briefly referred to in the preceding section, the degradation products of PP's are associated in varying degrees with thermal isomerization during the course of pyrolysis. Consequently, the configuration of the degradation products is not necessarily the same as that of the original polymer chain. The isomerization has been discussed in terms of the intramolecular stepwise radical-transfer processes.[5-10] In this section, its mechanism will be discussed on the basis of the pyrograms obtained.

The pyrolysis reaction is initiated by a random scission of the polymer backbone to give primary and secondary macroradicals (Scheme I). Provided PP decomposes only through such statistical chain cleavages, the relative yields of the products must be 25, 50, and 25% in each n-ad triplet (C_{3n-1}, C_{3n}, and C_{3n+1}) respectively as follows:

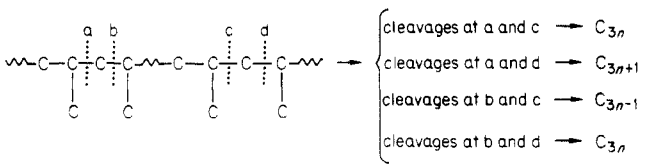

Scheme II

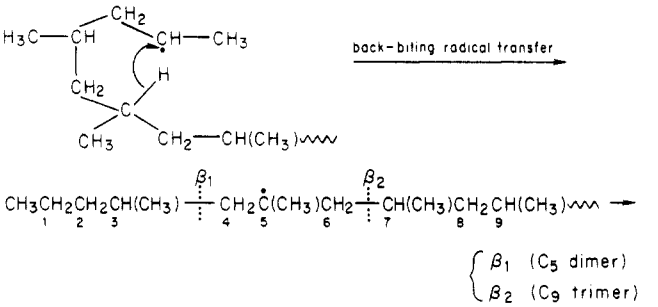

Scheme III

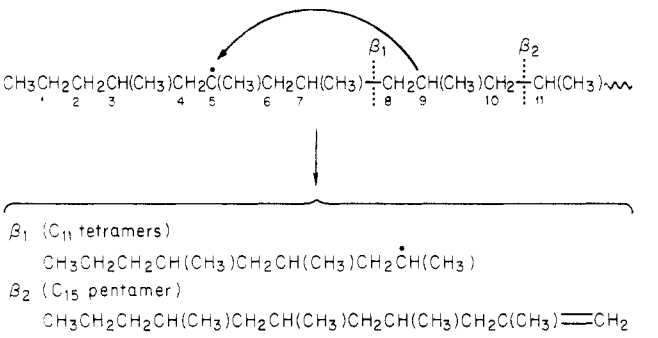

As shown in Figure 6, it is interesting to note that there exist general trends for the observed relative yields between C_{3n-1}, C_{3n}, and C_{3n+1} above hexamers ($n = 6$). The relative yields of C_{3n-1}, which have two end groups, **1**,

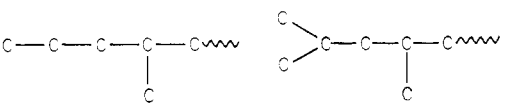

1 **2**

decrease as a monotonic function of molecular size and are always below the statistical value (25%). On the other hand, those of C_{3n+1} with two end groups, **2**, increase as the rise of molecular size and are always far above 25%. Those of C_{3n}, the end groups of which are composed of **1** and **2**, are close to the statistical value (50%) irrespective of the molecular size. These data clearly suggest that specific intramolecular radical transfer mostly followed by β-scission is contributing to the pyrolysis of PP in addition to the statistical random cleavage and that the contribution of the nonstatistical cleavage differs depending on the nature of the end groups of the resulting products. Moreover, these data indicate that the degradation products associated with the primary macroradical are the most stable.

In the same way as the thermal degradation of PE,[18] the most probable intramolecular radical transfer is expected to occur at the fifth carbon from the terminal of the macroradical by the back-biting mechanism through a six-membered ring intermediate. Of the two kinds of the macroradicals, the secondary one is particularly apt to transfer to the fifth carbon because the hydrogen atom attached to the teritary carbon is more reactive than that attached to the fifth secondary carbon of the primary radical[5] (Scheme II). The intermediate tertiary macroradicals thus formed yield mostly dimer (C_5) and trimer (C_9) through β-scission. If the intermediate tertiary macroradical is formed at the ninth carbon by successive back-biting, the most probable resulting products become tetramer (C_{11}) and pentamer (C_{15}) through β-scission (Scheme III).

Table VII
Relative Peak Intensities among C_{14}, C_{15}, and C_{16}

sample	relative peak intensities, %		
	C_{14}	C_{15}	C_{16}
PP-I(A)	12.9	64.0	23.1
PP-I(B)	13.8	64.4	21.8
PP-II	13.6	63.6	22.7
PP-III(A)	13.5	64.9	21.5
PP-III(B)	13.0	64.9	22.1
PP-III(C)	12.3	64.9	22.8
PP-III(D)	11.0	67.1	21.9

As shown in Scheme III, the resulting intermediates are a secondary radical for C_{11} and a stable monoolefin with a terminal double bond for C_{15}. The former still has some probability to dissociate into smaller products before stabilization through hydrogenation, while the latter only yields a saturated C_{15} product through hydrogenation. This mechanism may be the main reason why the relative yields of the C_{15} product in Table VII are always above the statistical value (50%) with all the PP samples.

The stereoisomerization during the pyrolysis of PP has been explained by the stereochemistry of the associated intermediates.[7] Each carbon atom in the backbone chain of PP is located in a tetrahedral arrangement composed of four sp^3 hybridized orbitals.

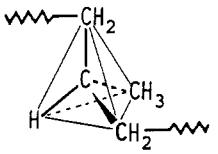

However, the intermediate tertiary radical is known to have a planar conformation composed of three sp^2 hybridized orbitals with an unpaired electron in a π-orbital which is perpendicular to the plane.

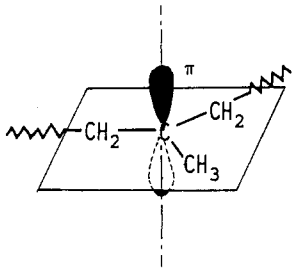

When the tertiary radical reverts to the tetrahedral arrangement, mainly by the back-biting mechanism, there exists an equal chance for a hydrogen atom to be abstracted on each side of the plane composed of the three sp^2 orbitals. Therefore, in this case equal amounts of the corresponding diastereoisomers are expected, irrespective of the original configuration. For example, from a long isotactic chain the following diastereoisomers are expected to be formed for C_{11} and C_{15} through stepwise back biting of the starting secondary macroradical, first to the 5th and then to the 9th carbon followed by β-scission (Scheme IV).

The fact that the relative yield (28.8%) of rr-C_{15} in Table III is much greater than that of mr-C_{15} (8.3%) for the highly isotactic sample PP-I(A) may be chiefly attributed to the specific mechanism for the stereoisomerization. On the other hand, the fact that the yield of mr-C_{14} (19.0%) for PP-I(A) is almost comparable with that of rr-C_{14} (14.4%) suggests that the starting secondary macroradical has a fairly high probability of transferring stepwise first to the 7th and then to the 11th carbon followed by β-scission to yield the mr-C_{14} in addition to the stepwise transfer first to the 5th and then to the 11th carbon to yield the rr-C_{14}.

Scheme IV

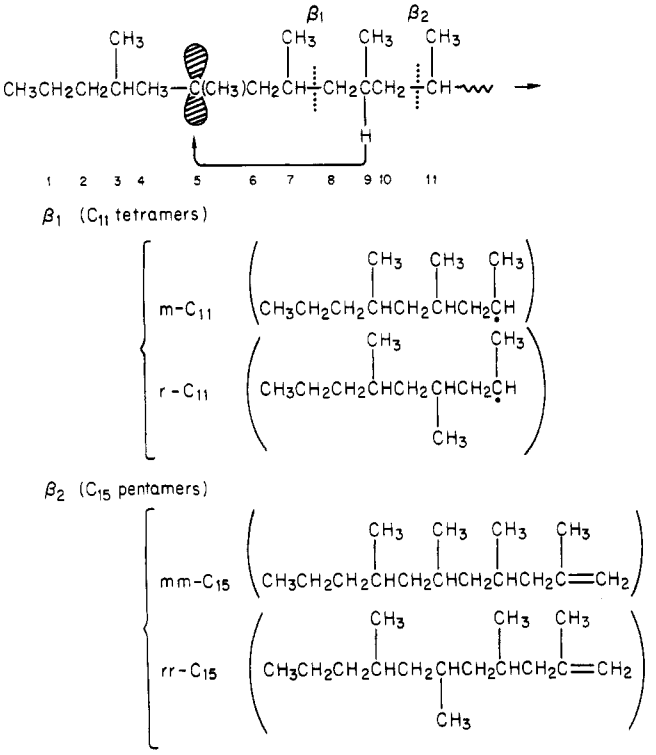

The primary macroradical shown in Scheme I has little possibility of transferring to the 5th carbon, however, because the associated hydrogen atoms are less reactive than those attached to tertiary carbons. Even if the transfer occurs at the fifth carbon, the resulting configuration of the intermediate macroradical does not cause any stereoisomerization because the fifth carbon is not asymmetric. This behavior of the primary macroradical is related to the fact that the degradation products associated with it are always formed far above the statistical value (25%) (Figure 6). The observation that the values for C_{13} dyads in Table II and C_{16} triads in Table III best correspond to the original stereoregularities is mostly attributed to the fact that the end groups of the C_{13} dyads and the C_{16} triads are related to the structure of the primary macroradical.

However, the fact that the observed yield of r-C_{13} (11.8%) for PP-I(A) in Table II is larger than the r content (4.6%) determined by ^{13}C NMR suggests that the starting primary macroradical with a long isotactic sequence partially transfers stepwise first to the fourth tertiary and then to the eighth tertiary carbon, followed by β-scission. Similarly, the reason that the observed yields of rr-C_{16} (12.5%) for PP-I(A) in Table III are larger than the rr content (2.8%) by ^{13}C NMR has to be explained by another specific transfer of the starting primary macroradical, first to the 6th tertiary and then to the 10th tertiary carbon followed by β-scission.

Peak Assignment of the Diastereoisomers in the Hexamer Region (C_{17}–C_{19}). In previous papers,[7,11] the peak assignments of the diastereoisomers formed from PP's were reported for tetramers (C_{11}–C_{13}) and pentamers (C_{14}–C_{16}). As was anticipated from the possible combinations of the monomer units, the tetramers were composed of six diastereoisomers (triplet of doublets), while the pentamers consisted of 10 components. Simiarly, as shown in Table VIII, the hexamers (C_{17}–C_{19}) were theo-

Table VIII
Possible Diastereoisomers for Hexamers (C_{17}-C_{19})

	structure	peak no.
C_{17}	mmm	1
	mmr	2
	mrm	3
	rmr	4
	rrm	5
	rrr	6
C_{18}	mmm	7
	rmm	8
	mmr	9
	mrm	10
	rmr	11
	rrm	12
	mrr	13
	rrr	14
C_{19}	mmm	15
	mmr	16
	mrm	17
	rmr	18
	rrm	19
	rrr	20

retically expected to be composed of 20 components. However, with a conventional glass capillary column, the efficiency was not great enough to separate the multiplets which bear a close resemblance to one another.

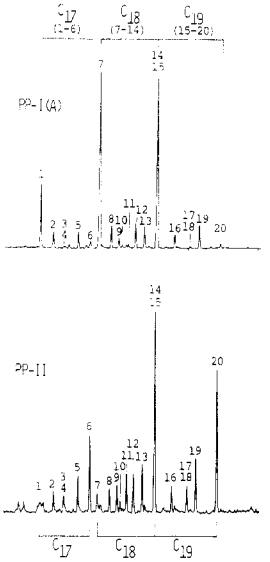

Figure 7. Peak assignments in the hexamer region (C_{17}–C_{19}) for PP-I(A) and PP-II; peak numbers correspond to those in Table VIII.

In this work, the multiplets were separated almost completely by use of the high-resolution fused-silica capillary column. Therefore, the peak assignment of the associated diastereoisomers in the hexamer region were carried out on the basis of the following empirical rules derived from the observed pyrograms of PP's with different stereoregularities: (1) The more racemic structures a product contains, the higher boiling point, i.e., the longer retention time it has. (2) Stereoisomerization at the symmetric carbon adjacent to an isopropyl-type end group takes place only with difficulty during pyrolysis. (3) Stereoisomerization rarely happens at more than two asymmetric carbons when a given degradation product is formed.

Figure 7 shows the observed partial pyrograms in the hexamer region for a highly isotactic PP-I(A) and a highly syndiotactic PP-II. Among three clusters of multiplets for C_{17}, C_{18}, and C_{19}, that of C_{17} is completely separated from that of C_{18}. However, those for C_{18} and C_{19} happened to overlap at rrr-C_{18} and mmm-C_{19} even by this high-resolution column. Relatively strong mrm and rmr peaks on the pyrogram of PP-II are responsible for the more heterotactic nature of PP-II than of PP-I(A) (mr-C_{16}, 24.7 and 5.4%, respectively, in Table III).

Acknowledgment. We are grateful to T. Usami, Plastic Research Laboratory, Mitsubishi Petrochemical Co., Ltd., for most helpful discussions.

Registry No. Polypropylene (homopolymer), 9003-07-0; isotactic polypropylene (homopolymer), 25085-53-4; syndiotactic polypropylene (homopolymer), 26063-22-9.

References and Notes

(1) Inoue, Y.; Nishioka, A.; Chujo, R. *Makromol. Chem.* **1972**, *152*, 15.
(2) Zambelli, A.; Dorman, D. E.; Richard Brewster, A. I.; Bovey, F. A. *Macromolecules* **1973**, *6*, 925.
(3) Randall, J. C. *J. Polym. Sci., Polym. Phys. Ed.* **1974**, *12*, 703.
(4) Zambelli, A.; Locatelli, P.; Bajo, G.; Bovey, F. A. *Macromolecules* **1975**, *8*, 687.
(5) Tsuchiya, Y.; Sumi, K. *J. Polym. Sci., Part A-1* **1969**, *7* 1599.
(6) Audisio, G.; Bajo, G. *Makromol. Chem.* **1975**, *176*, 991.
(7) Seeger, M.; Cantow, H.-J. *Makromol. Chem.* **1975**, *176*, 2059.
(8) Kiran, E.; Gillham, K. *J. Appl. Polym. Sci.* **1976**, *20*, 2045.
(9) Kiang, J. K. Y.; Uden, P. C.; Chien, J. C. W. *Polym. Degradation Stab.* **1980**, *2*, 113.
(10) Dickens, B. *J. Polym. Sci., Polym. Chem. Ed.* **1982**, *20*, 1169.
(11) Sugimura, Y.; Nagaya, T.; Tsuge, S.; Murata, T.; Takeda, T. *Macromolecules* **1980**, *13*, 928.

(12) Ogawa, T.; Elias, H.-G. *J. Macromol. Sci., Chem.* **1982**, *A17*, 727.
(13) Tsuge, S.; Sugimura, Y.; Nagaya, T. *J. Anal. Appl. Pyrolysis* **1980**, *1*, 221.
(14) Coleman, B. D.; Fox, T. G. *J. Polym. Sci., Part A* **1963**, *A1*, 3183.
(15) Zambelli, A.; Wolfgruber, C.; Zannoni, G.; Bovey, F. A. *Macromolecules* **1974**, *7*, 750.
(16) Doi, Y. Macromolecules **1979**, *12*, 248.
(17) Seno, H.; Tsuge, S.; Takeuchi, T. *Makromol. Chem.* **1972**, *161*, 185.
(18) Tsuchiya, Y.; Sumi, K. *J. Polym. Sci., Part B* **1968**, *6*, 357.

Tetrad Distribution of an Aromatic Copolyterephthalate by ^{1}H NMR

Marek Matlengiewicz

Institute of Polymer Chemistry, Polish Academy of Sciences, PL-41800 Zabrze, Poland.
Received February 23, 1983

ABSTRACT: A method for the complete analysis of the compositional tetrad distribution of 3,3′-dimethylbisphenol A–phenolphthalein copolyterephthalate (PDT/FT) by ^{1}H NMR spectroscopy with a lanthanide-shift reagent is presented. The signal of the terephthalic protons in the 100-MHz ^{1}H NMR spectrum of the copolyterephthalate recorded in the presence of Eu(fod)$_3$ has been found to exhibit separate lines for compositional tetrads. A theoretical model of the tetrad signal spectrum has been proposed, and computer simulation has been performed to calculate probabilities of the tetrads. The data obtained for an equimolar PDT/FT copolymer synthesized at 240 °C indicate significant deviation from a random distribution of comonomer units with a tendency to form block segments along the copolymer chain.

Determination of the comonomer sequence distribution of copolyterephthalates by means of ^{1}H NMR spectroscopy has been shown to be possible utilizing for the analysis the signals of the terephthalic protons.[1-3] However, the standard ^{1}H NMR spectra, up to 100 MHz, can be successfully used for the analysis in those few cases when comonomers are sufficiently different from one another, and as far as it is known comonomer sequences longer than dyads have not yet been recorded. In the case of a fully aromatic copolyterephthalate the standard spectra are useless for this purpose because the terephthalic signals of each homosequence occupy nearly the same position at about 8.40 ppm. The standard 100-MHz ^{1}H NMR spectra of the aromatic copolyterephthalate obtained from terephthaloyl chloride, being an intermonomer, and equimolar amounts of 3,3′-dimethylbisphenol A and phenolphthalein as comonomers (PDT/FT) were found to be useless for sequence analysis because terephthalic signals of PDT/FT as well as the signals of corresponding homopolyterephthalates exhibit a single terephthalic signal at 8.36 ppm (Figure 1). Application of Eu(fod)$_3$ lanthanide shift reagent was found to be a useful method for separating the terephthalic proton singlet of PDT/FT into signals of three compositional dyads,[3] while the methyl signal of a D unit in the PDT/FT chain was found to show only traces of splitting into signals of compositional triads.[4]

Since the PDT/FT copolymer is derived from symmetrical monomers which can be incorporated in only one way into the polymer chain, there is no head-to-head and head-to-tail isomerism. The small anisotropic effect of the phenolphthalein unit

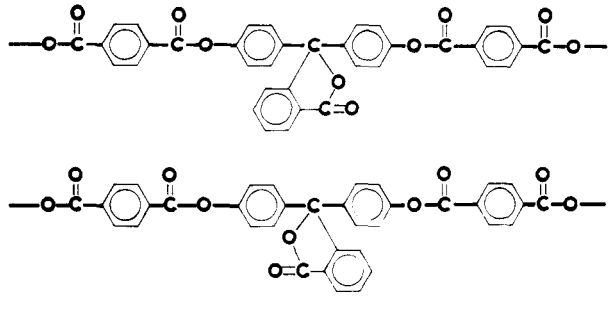

can also be neglected as shown by investigations of the homopolyterephthalate of phenolphthalein.[4] Hence, configurational sequences need not be taken into account. Differences in the copolyterephthalate microstructure are due only to comonomer unit distribution while the intermonomer units introduce no differentiation and can be omitted in the description for the sake of clarity. Henceforth the term "sequence" stands for compositional sequence.

Experimental Section

3,3′-Dimethylbisphenol A/phenolphthalein copolyterephthalate (50:50) (PDT/FT) was prepared at 240 °C by polycondensation of terephthaloyl chloride (Fluka AG) as intermonomer and equimolar amounts of 3,3′-dimethylbisphenol A and phenolphthalein (POCh, Poland) as comonomers in solution of redistilled α-chloronaphthalene (Reachim, USSR) under an argon atmosphere.

The molecular weight of the sample was about 16 000 as determined in THF by the Knauer vapor pressure osmometer and the Waters Associates Instruments ALC/GPC-202/401 chromatograph. Thus, the degree of polymerization was about 45 since for the equimolar PDT/FT copolymer sample, an average molecular weight of the repeating unit, $\bar{m}$, can be calculated according to

$$\bar{m} = (M_{-D-} + 2M_{-T-} + M_{-F-})/2 \quad (1)$$

where M_{-D-}, M_{-T-}, and M_{-F-} are the molecular weights of the 3,3′-dimethylbisphenol A, terephthalic, and phenolphthalein units in the chain, respectively.

^{1}H NMR spectra were recorded on a Varian 100-MHz XL-100 spectrometer by using 5 wt % solutions in $CDCl_3$ (Merck) at room temperature. Eu(fod)$_3$ (Fluka AG) was used as a lanthanide shift reagent (LSR).

Computer simulation of tetrad signals was performed by means of a Wang 2200 desk top computer equipped with a Wang 2212 X–Y plotter. The experimental spectra were compared with the simulated ones drawn by the plotter by means of a program for superposition of 28 Lorentzian–Gaussian lines.

Recording of Tetrad Signals. At higher concentration of Eu(fod)$_3$, the highly resolved terephthalic proton signals

0024-9297/84/2217-0473$01.50/0 © 1984 American Chemical Society